Neuro-Oncology 14(9):1136–1145, 2012.
doi:10.1093/neuonc/nos139
Advance Access publication June 29, 2012

Signal transducer and activator of transcription 3 promotes angiogenesis and drives malignant progression in glioma

Tiffany A. Doucette, Ling-Yuan Kong, Yuhui Yang, Sherise D. Ferguson, Jinbo Yang, Jun Wei, Wei Qiao, Gregory N. Fuller, Krishna P. Bhat, Kenneth Aldape, Waldemar Priebe, Oliver Bögler, Amy B. Heimberger, and Ganesh Rao

Departments of Neurosurgery (T.A.D., L.-Y.K., Y.Y., S.D.F., J.W., O.B., A.B.H., G.R.), Pathology (G.N.F., K.P.B., K.A.), and Biostatistics (W.Q.), the Brain Tumor Center (T.A.D., L.-Y.K., Y.Y., S.D.F., J.W., K.P.B., K.A., O.B., A.B.H., G.R.), and Experimental Therapeutics, The University of Texas MD Anderson Cancer Center, Houston, Texas (W.P.) and Lerner Research Institute, Cleveland Clinic, Cleveland, Ohio (J.Y.)

Signal transducer and activator of transcription (STAT) 3 has been described as a "master regulator" of signaling pathways involved in the transition from low-grade glioma (LGG) to high-grade glioma (HGG). Although STAT3 is overexpressed in HGGs, it remains unclear whether its overexpression is sufficient to induce or promote the malignant progression of glioma. To characterize the effect of STAT3 expression on tumor progression in vivo, we expressed the *STAT3* gene in glioneuronal progenitor cells in mice. *STAT3* was expressed alone or concurrently with platelet-derived growth factor B (*PDGFB*), a well-described initiator of LGG. STAT3 alone was insufficient to induce tumor formation; however, coexpression of STAT3 with PDGFB in mice resulted in a significantly higher incidence of HGGs than PDGFB alone. The median symptomatic tumor latency in mice coexpressing STAT3 and PDGFB was significantly shorter, and mice that developed symptomatic tumors demonstrated significantly higher expression of phosphorylated STAT3 intratumorally. In HGGs, expression of STAT3 was associated with suppression of apoptosis and an increase in tumor cell proliferation. HGGs induced by STAT3 and PDGFB also displayed frequent foci of necrosis and microvascular proliferation. The expression of CD31 (a marker of endothelial proliferation) was significantly higher in tumors induced by coexpression of STAT3 and PDGFB. When mice injected with PDGFB and STAT3 were treated with a STAT3 inhibitor, median survival increased and the incidence of HGG and CD31 expression decreased significantly. These results demonstrate that *STAT3* promotes the malignant progression of glioma. Inhibiting STAT3 expression mitigates tumor progression and improves survival, validating it as a therapeutic target.

Keywords: glioma, mesenchymal, mouse model, proneural, STAT3.

Gliomas are the most common primary brain tumor in humans and constitute a range of tumor types, including indolent-appearing lesions that inexorably progress to more aggressive tumors, which are associated with shorter survival in patients. Patients with low-grade gliomas (LGGs) have an overall survival time of 7–10 years, but as these tumors devolve to more malignant, high-grade gliomas (HGGs), the overall survival time decreases to 1–3 years.[1–4] The WHO grading system for gliomas is based on the identification of specific histologic features, including necrosis, microvascular proliferation, and brisk mitotic activity.[5] Identifying the key genetic contributors that result in tumor progression is the focus of intense investigation because inhibition of their activity may mitigate the malignant degeneration of glioma. Activation of the platelet-derived growth factor (PDGF) signaling pathway initiates gliomagenesis.[6] In human gliomas, the PDGF receptor (PDGFR) is commonly overexpressed, and increased expression correlates with higher tumor grade.[7,8] Overexpression of the PDGFR ligand PDGFB results predominantly in LGGs

Received March 2, 2012; accepted May 18, 2012.

Corresponding Authors: Ganesh Rao, MD, Department of Neurosurgery, Unit 442, The University of Texas MD Anderson Cancer Center, 1515 Holcombe Blvd., Houston, TX 77030 (grao@mdanderson.org); Amy B. Heimberger, MD, Department of Neurosurgery, Unit 442, The University of Texas MD Anderson Cancer Center, 1515 Holcombe Blvd., Houston, TX 77030 (aheimber@mdanderson.org).

in murine models,[9–11] and PDGFB can cooperate with other signaling molecules to enhance tumor formation and progression.[12–14] Similarly, signal transducer and activator of transcription (STAT) 3 is a key candidate for causing the malignant progression of glioma, given its role in tumorigenesis,[15] its frequent expression in HGGs but not in LGGs, and its designation as a negative prognostic factor for survival in patients with glioma.[16] Phosphorylated (p)STAT3 leads to transcriptional activation of downstream genes involved in processes such as cell proliferation, suppression of apoptosis, and angiogenesis.[17,18] *STAT3* expression is also suspected to promote the mesenchymal phenotype of HGG, which is associated with a poor clinical outcome in patients.[19] Furthermore, STAT3 has been shown to maintain the proliferation and multipotency of glioma cancer stem cells.[20] However, to date no in vivo studies have been performed to elucidate the role of STAT3 in malignant progression of glioma.

To determine whether *STAT3* contributes to the formation of HGGs in vivo, we studied the effect of *STAT3* expression in glioneuronal progenitor cells using the RCAS (replication-competent ASLV long terminal repeat with a splice acceptor)/Ntv-a transgenic mouse system.[21] Here, we show that when coexpressed with PDGFB, STAT3 promotes the malignant progression of glioma by generating tumors with marked microvascular proliferation and necrosis. STAT3-driven tumors also show a suppression of apoptosis, resulting in a commensurate increase in tumor cell proliferation. Conversely, inhibition of STAT3 reverses the angiogenic effect of STAT3, decreases the proportion of HGGs, and leads to longer survival in the mice.

Materials and Methods

Vector Constructs

To study the effect of STAT3 in conjunction with PDGFB-dependent glioma formation in vivo, the human *STAT3* gene was expressed in mice using the RCAS/Ntv-a transgenic mouse system.[22] The generation of RCAS-PDGFB, which was constructed with a hemagglutinin (HA) epitope tag, has been previously described,[11] and RCAS-PDGFB was a gift of Dr Wei Zhang (The University of Texas MD Anderson Cancer Center). RCAS-STAT3 was generated by amplifying the sequence encoding the cDNA by PCR using specially designed primers that enable directional cloning into a Gateway entry vector. The proprietary Gateway LR recombination reaction between the entry vector containing our gene of interest and a previously constructed RCAS destination vector resulted in the desired RCAS vector, which was then verified by sequencing.

Transfection of DF-1 Cells

DF-1 immortalized chicken fibroblasts were grown in Dulbecco's modified Eagle's medium with 10% fetal bovine serum (Gibco) in a humidified atmosphere of 95% air/5% CO_2 at 37°C. Live virus was produced by transfecting plasmid versions of RCAS vectors into DF-1 cells using FuGene6 (Roche). These cells were then replicated in culture.

Immunofluorescence

To verify STAT3 expression, untransfected DF-1 cells were grown in culture, transfected with RCAS-STAT3, and allowed to replicate for 2 to 3 passages (Supplementary material, Fig. S1A and B). Cells were then fixed with 4% paraformaldehyde in phosphate buffered saline (PBS), followed by treatment with cold methanol. Immunocytochemical labeling was performed using standard methods. A rabbit polyclonal antibody against STAT3 (1:100; Cell Signaling Technology) and goat anti-rabbit Alexa Fluor 594 fluorescent conjugate (1:500; Molecular Probes) were used for detection. Prolong Gold antifade reagent with 4′-6-diamidino-2-phenylindole (DAPI) (Molecular Probes) was used for labeling cell nuclei. Staining was visualized with a Zeiss Axioskop 40 microscope (Supplementary material, Fig. 1A).

Western Blot Analysis

Verification of STAT3 expression from DF-1 cells after transfection was performed by Western blotting (Supplementary material, Fig. 1B). Whole-cell lysates were prepared from DF-1 untransfected cultures and DF-1 cells transfected with RCAS-PDGFB or RCAS-STAT3. Protein samples (10 μg) were fractionated by sodium dodecyl sulfate polyacrylamide gel electrophoresis using gels containing 10% polyacrylamide, transferred to a polyvinylidene difluoride membrane, and probed with the anti-HA antibody (1:1000; F7, Santa Cruz Biotechnology) to detect PDGFB expression, anti-STAT3 (1:1000; 9132, Cell Signaling Technology) for total STAT3 expression, or anti-pSTAT3 (1:2000; 9145, Cell Signaling Technology) for pSTAT3 expression. Secondary antibodies used for detection were goat anti-mouse immunoglobulin (Ig)G (1:2500; Pierce) and goat anti-rabbit IgG (1:10,000). The blots were developed using the ECL Plus detection kit (GE Healthcare) following the manufacturer's protocol.

In vivo Somatic Cell Transfer in Transgenic Mice

Generation of the transgenic Ntv-a mouse has been previously described.[22] The mice are hybrids of multiple strains: C57BL/6, BALB/c, FVB/N, and cluster of differentiation (CD)1. To transfer genes via RCAS vectors, defined volumes of DF-1 producer cells transfected with a particular RCAS vector (1×10^4 DF-1 cells in 1–2 μL of PBS) were injected into the frontal lobes of Ntv-a mice, anterior to the coronal suture of the skull, using a 10-μL gastight Hamilton syringe. The mice were injected within 24–48 h after birth because the population of nestin+ cells producing TVA is highest during this period. Equal numbers of

DF-1 cells were injected in the cohorts of animals that received 2 RCAS vectors. The mice were killed 90 days after injection, or sooner if they demonstrated morbidity related to tumor burden, including hydrocephalus or debility. Their brains were removed and analyzed for tumor formation. Histologic verification of tumor formation and determination of glioma type (LGG or HGG) was performed by the study neuropathologist (G.N.F.). High-grade tumors were differentiated by the presence of microvascular proliferation and/or foci of necrosis. The animal experiments described in this research were approved by the Institutional Animal Care and Use Committee at The University of Texas MD Anderson Cancer Center (Protocols 08-06-11632 and 08-06-11832).

Reverse Transcriptase–PCR

To verify expression of STAT3 after incorporation into the host cell DNA in tumor sections, we performed reverse transcriptase (RT)-PCR on the brains of mice injected with RCAS-STAT3 ($N = 3$) . After the mice were killed, their forebrains were removed and frozen in liquid nitrogen. Tissue specimens were homogenized, and RNA was extracted. The primer sequences for STAT3 were 5′ AACTCTCACGGACGAGGAGCT 3′ and 5′ AGTAGTGAACTGGACGCCGG 3′. The PCR products were separated by gel electrophoresis. The bands observed on the gels verified incorporation of the *STAT3* gene into brain cells of injected mice (Supplementary material, Fig. 2).

Treatment Schema

WP1066 was dissolved in dimethylsulfoxide (DMSO; Sigma-Aldrich), then mixed with polyethylene glycol (PEG)300 (ratio, 1:4; Sigma-Aldrich) to the desired concentration. A cohort of newborn Ntv-a mice ($N = 19$) was injected with the RCAS-*PDGFB* + RCAS-*STAT3* constructs. Twenty-one days after introduction of the glioma-inducing transgenes, treatment was started with WP1066 (30 mg/kg × 3 wk), administered by oral gavage in a vehicle of DMSO/PEG300 (20 parts/80 parts) on Monday, Wednesday, and Friday for a total of 3 weeks. The 30 mg/kg dosing regimen was selected based on the toxicity studies performed that established this as the level of no observed adverse effect. The mice were killed 90 days after injection, or sooner if they demonstrated morbidity related to tumor burden, including hydrocephalus or debility. To compare M2 macrophage infiltration and pSTAT3 immunostaining in the different injection sets, a separate cohort of mice injected with RCAS-*PDGFB* + RCAS-*STAT3* was analyzed.

Immunohistochemistry

Mouse brains were paraffin embedded, and 4-μm brain sections were used for immunohistochemical analysis. The Thermo Scientific PT Module (Thermo Fisher Scientific) with citrate buffer was used for antigen retrieval. Staining was performed using the Lab Vision Immunohistochemical Autostainer 360 (Thermo Fisher Scientific). Immunoreactive staining was visualized using an avidin–biotin complex technique with diaminobenzidine (Invitrogen) as the chromogenic substrate and hematoxylin as the counterstain. To detect pSTAT3 expression, we used a primary monoclonal antibody against Tyr705 pSTAT3 (1:50; Cell Signaling Technology). To detect apoptosis, we used a primary antibody against cleaved caspase 3 (1:50; Cell Signaling Technology), an indicator of both mitochondria-mediated (intrinsic) and death receptor-mediated (extrinsic) apoptosis. An antibody against phosphohistone H3 (pHH3; 1:1000; Millipore) was used to assess the extent of mitotic activity, as an indicator of cell proliferation. An antibody against Olig2 (1:500; Millipore) was used to characterize the proneural phenotype of tumors, and antibodies against CD31 (1:400; R&D Systems) and vascular epithelial growth factor (VEGF; 1:100; Millipore) were used to characterize microvascular proliferation and the mesenchymal phenotype.

Quantification of pSTAT3 Expression in Tumors

To detect and quantify the expression of pSTAT3 in the different injection sets, we immunostained formalin-fixed, paraffin-embedded tumor-bearing tissue sections with an antibody against pSTAT3. We counted the total number of cells and the number of positively stained cells in the areas of highest tumor cell density in 10 nonoverlapping high-power (400×) microscopic fields in tumor-bearing brains taken from 3–5 mice in each injection set (cell counts were performed by T.D., Y.Y., and G.R.). The pSTAT3 expression level was calculated as the percentage of positive cells in each field. The median total number of cells counted was 1875 (range, 783–4085).

We also assessed the association between pSTAT3 expression level and survival time. Tumor-bearing mice were divided into 2 groups: long-term survivors (≥90 days) and short-term survivors (those killed before 90 days due to symptomatic tumor formation). For this analysis, tumor-bearing brains were taken from 5 mice in each injection set. The median total number of cells counted in the RCAS-*PDGFB* injection set for short-term survivors was 1292 (range, 740–5057); and for long-term survivors, 1050 (range, 548–1506). The corresponding numbers in the RCAS-*PDGFB* + RCAS-*STAT3* injection set were 1072 (range, 481–1996) and 1111 (range, 651–1479).

Mitotic Index

To detect and quantify mitotic activity in the different injection sets, we analyzed formalin-fixed, paraffin-embedded tumor-bearing tissue sections with an antibody against pHH3, which has been described as a useful marker for determining the mitotic index in gliomas.[23] We counted the total number of cells and the number of positively stained cells in the area of highest tumor cell

density in 10 nonoverlapping high-power (400×) microscopic fields in tumor-bearing brains taken from 5 mice in each injection set. The mitotic index was calculated as the percentage of positive cells in each field. The median total number of cells counted per field was 1771 (range, 999–2871).

Apoptotic Assay

Apoptosis was detected and quantified in the different injection sets by immunostaining formalin-fixed, paraffin-embedded tumor-bearing tissue sections with an antibody against cleavage of caspase 3, which is an early and consistent signaling event in apoptosis and can be used to determine the apoptotic index.[24] We counted the total number of cells and the number of positively stained cells in the area of highest tumor cell density in 10 nonoverlapping high-power (400×) microscopic fields in tumor-bearing brains taken from 3 mice in each injection set. The apoptotic index was calculated as the percentage of positive cells in each field. The median total number of cells counted per field was 1298 (range, 765–3641).

Phenotypic Characterization of Tumor

To determine the phenotype of tumors generated in the Ntv-a mice after injection of RCAS vectors, we analyzed the tumors for histologic features associated with the mesenchymal phenotype, including microvascular proliferation and necrosis. We immunostained formalin-fixed, paraffin-embedded tumor-bearing tissue sections with an antibody against Olig2, a marker of the proneural phenotype, and antibodies against CD31 and VEGF, markers of microvascular proliferation. We counted the total number of cells and the number of positively stained cells in the area of highest tumor cell density in 10 nonoverlapping high-power (400×) microscopic fields in tumor-bearing brains taken from 5 mice in each injection set. The expression level was calculated as the percentage of positive cells in each field. For CD31, the median number of cells counted in the RCAS-*PDGFB* injection set was 1032 (range, 769–2332) and, in the RCAS-*PDGFB* + RCAS-*STAT3* injection set, 1241 (range, 730–2281). For Olig2, the corresponding numbers were 1410 (range, 614–1891) and 2588 (range, 855–4394). In the cohort of mice treated with WP1066, we counted the total number of cells and the number of positively stained cells in the area of highest tumor cell density in 10 nonoverlapping high-power (400×) microscopic fields in tumor-bearing brains taken from 10 mice. The median number of cells counted was 1173 (range, 823–1498).

Statistical Analysis

Summary statistics were provided in the form of frequencies and percentages. The χ^2 test was used to compare the tumor incidence between the different injection sets. Kaplan–Meier curves were used to estimate unadjusted tumor latency. The log-rank test was used to compare the time-to-event variable between groups. To compare pHH3, cleaved caspase 3, Olig2, and CD31 expression between injection sets, we fit the linear mixed model to assess the percentage of positive cells, after adjusting for different injection sets and taking into account the associations among repeated measures within the same tumor. For the comparison of pSTAT3 positive cells between injection sets, the distribution of the percentage of positive cells was highly skewed; therefore, we used the logarithmic scale, log[positive/(positive + negative)], in this analysis. The Bonferroni method was used to adjust for multiple pairwise comparisons. All tests were 2-sided, and $P < .05$ was considered statistically significant. To compare pSTAT3 and F4/80 expression between treated and untreated cohorts, Student's *t*-test was used to compare the mean number of positive cells. Statistical analysis was carried out using SAS v.9 and Graphpad Prism v.5.03 software.

Results

STAT3 Cooperates with PDGFB to Promote Malignant Progression of Glioma

To evaluate the effect of STAT3 expression on glioma formation in vivo, we injected newborn Ntv-a mice with the RCAS-*STAT3* vector either alone or in conjunction with the RCAS-*PDGFB* vector. Within the 90-day observation period, gliomas were detected in the brains of 28 of 29 (97%) mice injected with RCAS-*PDGFB* alone and 38 of 38 (100%) mice injected with RCAS-*PDGFB* + RCAS-*STAT3* (Fig. 1). Tumors were not detected in any of the 24 mice injected with RCAS-*STAT3* alone. The incidence of HGGs, with histologic features of microvascular proliferation and/or

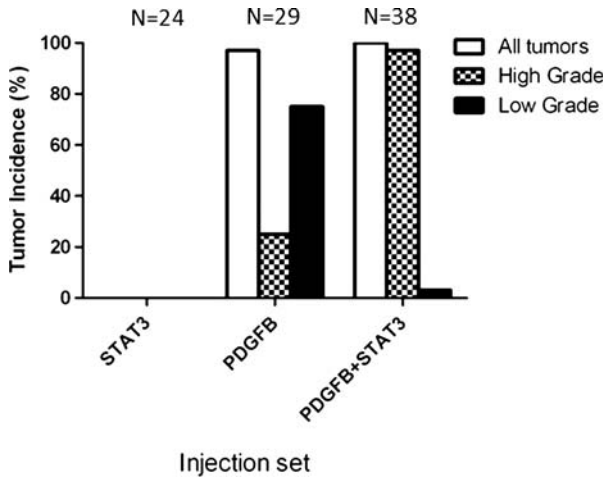

Fig. 1. The incidence of high-grade gliomas was significantly higher in mice injected with RCAS-*PDGFB* + RCAS-*STAT3* than in those injected with RCAS-*PDGFB* alone. RCAS-*STAT3* was insufficient to induce tumor formation.

Table 1. Tumor incidence and median tumor latency, by injection set

Injection Set	RCAS-STAT3	RCAS-PDGFB	RCAS-PDGFB + RCAS-*STAT3*
Tumor incidence, no. (%)	0/24 (0%)	28/29 (97%)	38/38 (100%)
High-grade glioma incidence, no. (%)	N/A	7/28 (25%)	36/38 (95%)
Low-grade glioma incidence, no. (%)	N/A	21/28 (75%)	2/38 (5%)
Tumor latency (days), median (range)	N/A	90 (29–90)	53 (20–90)

necrosis, was significantly higher in tumors induced by RCAS-*PDGFB* + RCAS-*STAT3* than in those induced by RCAS-*PDGFB* alone (χ^2 test, $P < .001$) (Table 1). The median tumor latency was significantly shorter in mice injected with RCAS-*PDGFB* + RCAS-*STAT3* than in those injected with RCAS-*PDGFB* alone (log-rank test, $P < .003$) (Fig. 2, Table 1), indicating that STAT3 cooperates with PDGFB to promote malignant progression.

pSTAT3 Expression Is Associated with Increased Glioma Grade and Decreased Survival Time

In LGGs, regardless of the injection vector, pSTAT3 expression was minimal. The median percentage of pSTAT3-positive cells was significantly higher in HGGs induced by RCAS-*PDGFB* + RCAS-*STAT3* than in those induced by RCAS-*PDGFB* alone (pairwise comparison, $P < .03$) (Fig. 3A, Table 2). Necrosis was identified in both RCAS-*PDGFB* and RCAS-*PDGFB* + RCAS-*STAT3* tumors. However, we observed necrosis in 13 of 38 RCAS-*PDGFB* + RCAS-*STAT3* tumors (34%), but in only 1 of 28 RCAS-*PDGFB* tumors (4%) (χ^2 test, $P = .012$). Furthermore, pSTAT3-expressing cells appeared to localize to regions of tumor necrosis in HGGs induced by RCAS-*PDGFB* + RCAS-*STAT3* but not in the single tumor induced by RCAS-*PDGFB* alone that displayed necrosis (Fig. 3B).

We also analyzed the association of pSTAT3 expression with survival time. Tumor-bearing mice from each injection set were divided into 2 groups: long-term survivors (≤90 days) and short-term survivors (those killed before 90 days due to symptomatic tumor formation). In the group injected with RCAS-*PDGFB* alone, presence of cells expressing pSTAT3 in tumors from long-term survivors was a mean of 2.6% (SEM 0.7%) compared with 12% (SEM 1.6%) in tumors from short-term survivors (mean estimates from linear mixed model, $P = .02$) (Fig. 3C). In the group injected with RCAS-*PDGFB* + RCAS-*STAT3*, presence of pSTAT3-positive cells in tumors from long-term survivors was a mean of 3.7% (SEM 1.3%) compared with 26.8% (SEM 2.2%) in tumors from short-term survivors (mean estimates from a linear mixed model, $P = .006$) (Fig. 3C).

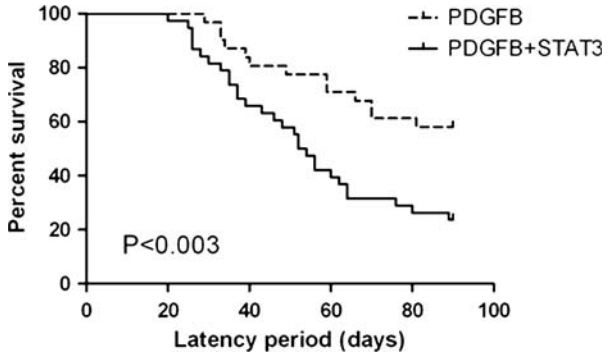

Fig. 2. The median tumor latency was significantly longer in mice injected with RCAS-*PDGFB* alone (90 days, range 29–90 days) than in those injected with RCAS-*PDGFB* + RCAS-*STAT3* (53 days, range 20–90 days).

STAT3 Suppresses Apoptosis, with a Concomitant Increase in Tumor Cell Proliferation

To ascertain the anti-apoptotic effect of STAT3 on glioma formation, we compared the apoptotic index, determined on the basis of staining tumors for cleaved caspase 3. To minimize the influence of grade, we selected only HGGs for analysis. The median apoptotic index was significantly higher in HGGs induced by RCAS-*PDGFB* alone than in those induced by RCAS-*PDGFB* + RCAS-*STAT3* (pairwise comparison, $P < .001$) (Fig. 4, Table 2). Next, we determined whether the observed reduction in apoptosis associated with STAT3 expression correlated with an increase in tumor cell proliferation. We compared the mitotic activity, determined on the basis of staining tumors for pHH3, between HGGs induced by RCAS-*PDGFB* + RCAS-*STAT3* and HGGs induced by RCAS-*PDGFB* alone. The median mitotic index in RCAS-*PDGFB* + RCAS-*STAT3* HGGs was significantly enhanced compared with that of RCAS-*PDGFB* HGGs (pairwise comparison, $P < .001$) (Fig. 4, Table 2), indicating that STAT3 increases tumor cell proliferation.

Histologic Characterization of Tumor Phenotype

We characterized the tumors induced by different injection sets by analyzing the expression of VEGF and CD31, markers of microvascular proliferation. HGGs induced by RCAS-*PDGFB* + RCAS-*STAT3* demonstrated much more conspicuous VEGF staining than HGGs induced by RCAS-*PDGFB* alone (Fig. 5A). We quantified the extent of CD31 staining in RCAS-*PDGFB* HGGs and RCAS-*PDGFB* + RCAS-*STAT3* HGGs (VEGF staining in the tumors was very diffuse and difficult to quantify). CD31 expression was significantly higher in the latter (mean, 4.2%; SEM,

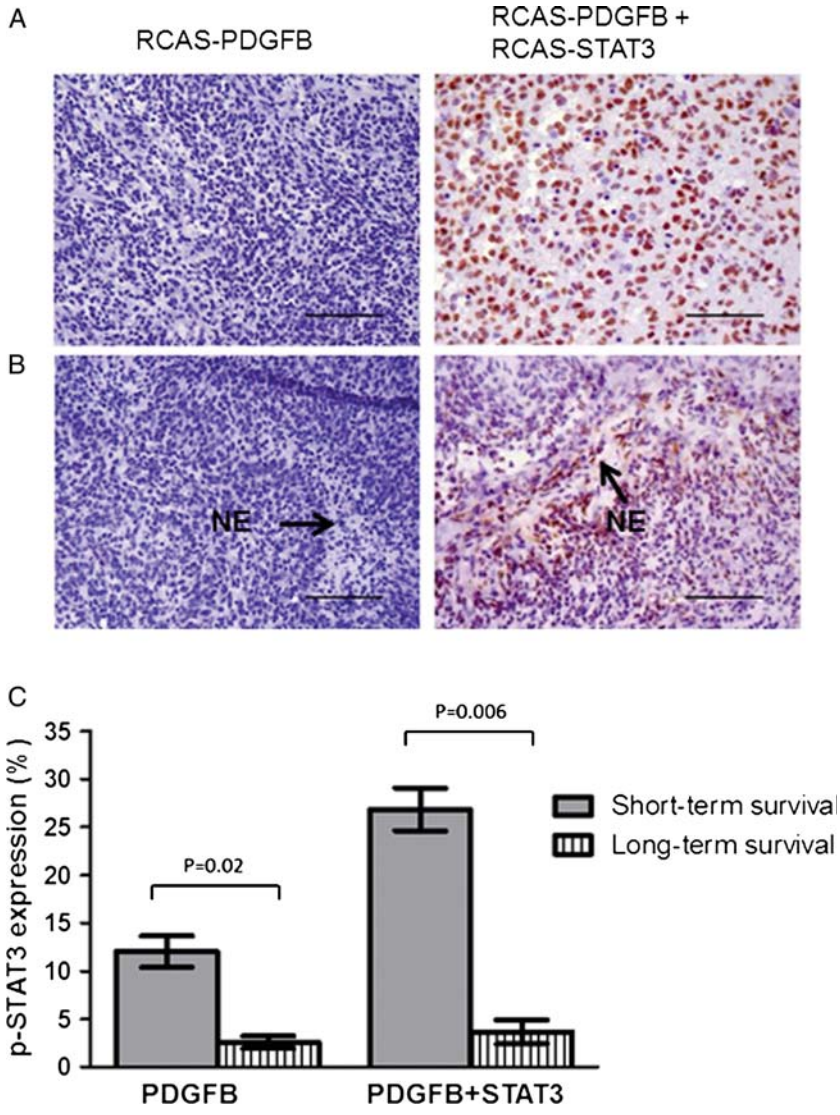

Fig. 3. Expression of pSTAT3 is increased in tumors induced by RCAS-*PDGFB* + RCAS-*STAT3* and pSTAT3-expressing cells appear to localize to areas of necrosis. (A) Photomicrograph (400× magnification) showing relatively minimal pSTAT3 expression in the nuclei within an HGG induced by RCAS-*PDGFB* compared with a tumor induced by RCAS-*PDGFB* + RCAS-*STAT3* (scale bar = 50 μm). (B) Photomicrograph (400×) showing pSTAT3-expressing cells preferentially localizing to areas of necrosis (denoted as NE) in HGGs induced by RCAS-*PDGFB* + RCAS-*STAT3* but not in the only HGG induced by RCAS-*PDGFB* alone that displayed necrosis (scale bar = 50 μm). (C) Percentage of cells expressing pSTAT3 in mice killed due to symptomatic tumor formation before the end of the 90-day observation period (labeled "short-term survival") compared with those who survived to 90 days (labeled "long-term survival") in RCAS-*PDGFB* (left) and RCAS-*PDGFB* + RCAS-*STAT3* (right) injection sets. Error bars indicate SEM.

Table 2. Median percentages of cells stained positive in high-grade tumors induced by RCAS-PDGFB or by RCAS-PDGFB + RCAS-STAT3

Injection Set	RCAS-PDGFB	RCAS-PDGFB + RCAS-STAT3
pSTAT3 expression	0.4% (0%–47%)	9.0% (0%–77%)
Mitotic index	1.0% (0.1%–2%)	3.6% (0%–9%)
Apoptotic index	0.6% (0%–7%)	0.2% (0%–3%)

The ranges are reported in parentheses.

1.1%) than in the former (mean, 0.6%, SEM, 0.2%; pairwise comparison, $P = .02$) (Fig. 5B). Because microvascular proliferation is a feature of the mesenchymal glioma phenotype, we also characterized the tumors by examining the expression of Olig2, a marker of the proneural glioma phenotype. Tumors induced by RCAS-*PDGFB* alone were homogenously positive for Olig2. However, tumors induced by RCAS-*PDGFB* + RCAS-*STAT3* displayed prominent areas of tumor that were devoid of Olig2 staining (Supplementary material, Fig. 3).

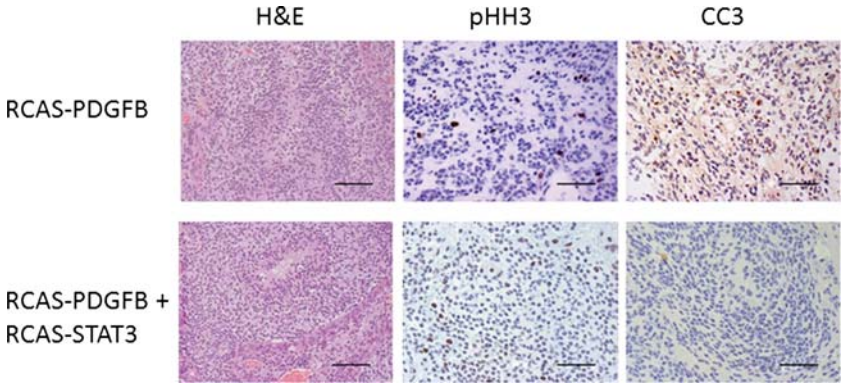

Fig. 4. STAT3 promotes tumor cell proliferation and suppression of apoptosis. Representative hematoxylin and eosin (H&E) photomicrographs (400× magnification) of HGGs induced by RCAS-*PDGFB* or by RCAS-*PDGFB* + RCAS-*STAT3*. These tumors were studied for expression of pHH3 as a marker of tumor cell proliferation and cleaved caspase 3 (CC3) as a marker of apoptosis. HGGs induced by RCAS-*PDGFB* + RCAS-*STAT3* showed higher expression of pHH3 and lower expression of CC3 compared with tumors induced by RCAS-*PDGFB* alone (scale bar = 50 μm).

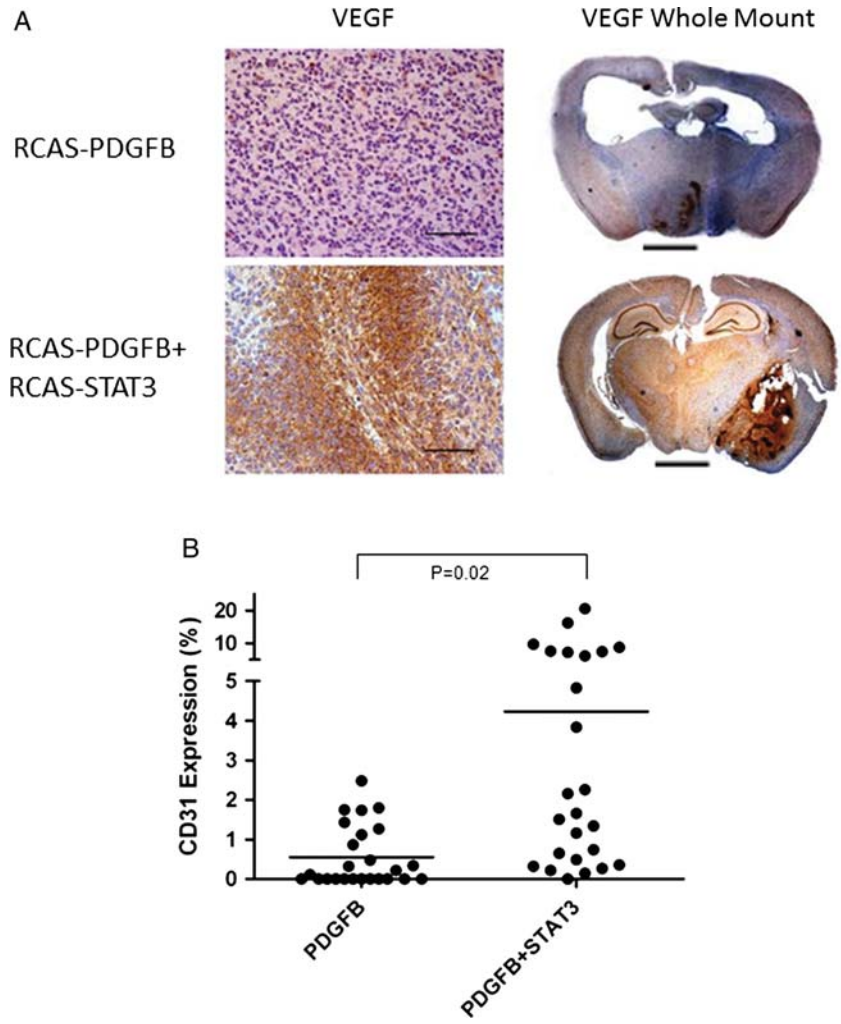

Fig. 5. Tumors induced by RCAS-*PDGFB* + RCAS-*STAT3* display increased microvascular proliferation. (A) Photomicrograph (400×) of VEGF staining in high-grade tumors induced by RCAS-*PDGFB* or by RCAS-*PDGFB* + RCAS-*STAT3*. Tumors induced by RCAS-*PDGFB* + RCAS-*STAT3* demonstrate large foci of VEGF staining throughout the tumor mass, whereas there is minimal staining in high-grade tumors induced by RCAS-*PDGFB* alone. Whole-mount photomicrograph (50×) of VEGF staining in a high-grade tumor, showing the localization of VEGF to the high-grade areas (areas surrounding necrosis or microvascular proliferation) (scale bar = 2.5 mm). (B) Expression of CD31 in tumors induced by RCAS-*PDGFB* or by RCAS-*PDGFB* + RCAS-*STAT3*. Horizontal lines indicate the mean.

Inhibition of STAT3 Decreases Microvascular Proliferation and M2 Macrophage Infiltration and Improves Survival

Because tumors induced by RCAS-*PDGFB* + RCAS-*STAT3* resulted in a higher proportion of HGGs, microvascular proliferation, and pSTAT3 expression, we used this model to study whether inhibition of STAT3 could mitigate the malignant transformation of tumors. A cohort of mice injected with RCAS-*PDGFB* + RCAS-*STAT3* ($N = 19$) was treated with WP1066, a well-described inhibitor of STAT3.[25] We observed tumors in 17 of 19 mice (89%). Of these tumors, 10 (59%) were HGGs, and 7 (41%) were LGGs. The percentage of HGGs in the mice after treatment with WP1066 was significantly lower than that of untreated mice from the original injection set (χ^2, $P < .0001$) (Fig. 6A). As expected, treatment with WP1066 significantly reduced expression of pSTAT3 (Supplementary material, Fig. 4). To ascertain the extent of WP1066 on suppressing microvascular proliferation we quantified CD31 expression in the treated mice. The expression of CD31 was significantly less in treated mice compared with untreated mice from the original injection set (linear mixed models, $P < .001$) (Fig. 6B). Inhibition of STAT3 also decreased the intratumoral infiltration of M2 macrophages (Supplementary material, Fig. 5). We have shown previously that increased M2 macrophage infiltration into the tumor correlates negatively with survival in both humans and mice.[25] Treated mice also demonstrated longer symptom-free survival (median, 90 days; range, 31–90 days). This was significantly longer than symptom-free survival (median, 53 days) observed in the mice injected with RCAS-*PDGFB* and RCAS-*STAT3* (log-rank test, $P = .0002$) (Fig. 6C).

Discussion

STAT3 expression has been associated with HGGs, but its relevance to tumor development is unclear. Recently we showed that *BCL2* enhances the malignant progression of glioma[12] and that inhibition of *STAT3* in a *BCL2*-dependent model of HGG yields a measurable therapeutic benefit.[25] Because *STAT3* lies upstream from *BCL2*, we investigated whether overexpression of *STAT3* influences glioma formation and progression and whether its inhibition would yield similar therapeutic effects as observed in our previous studies. *STAT3* was expressed in glioneuronal progenitor cells either alone or in conjunction with *PDGFB*, a known initiator of primarily LGG. We found that the incidence of high-

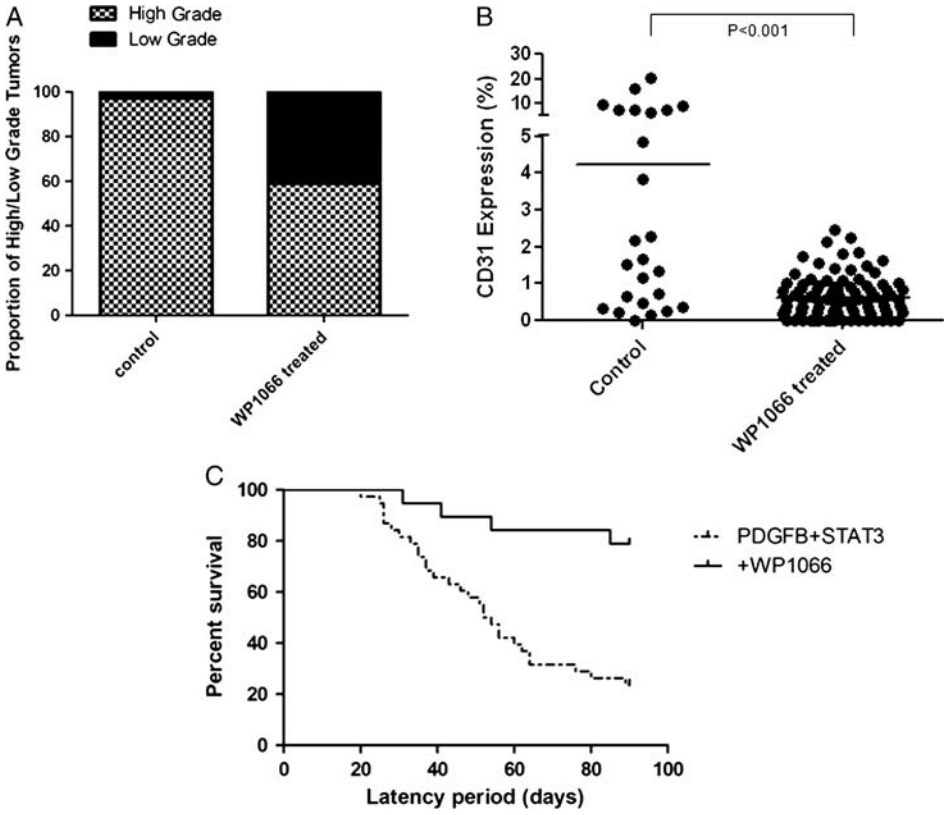

Fig. 6. Tumors induced by RCAS-*PDGFB* and RCAS-*STAT3* after treatment with WP1066. (A) WP1066 treatment decreases the percentage of high-grade gliomas compared with untreated RCAS-*PDGFB* + RCAS-*STAT3* injected mice (control). (B) WP1066 decreases microvascular proliferation as determined by staining for CD31 in tumors (horizontal line indicates the mean). (C) The median tumor latency was significantly longer in mice injected with RCAS-PDGFB + RCAS-STAT3 treated with WP1066 compared with the original group of untreated mice.

grade tumors was higher in mice overexpressing both *PDGFB* and *STAT3* than in those overexpressing *PDGFB* alone. Malignant progression and poorer symptom-free survival in tumor-bearing mice was associated with an increase in pSTAT3 expression. Tumors induced by coexpression of *PDGFB* and *STAT3* demonstrated characteristic histologic features of HGGs, including necrosis and microvascular proliferation. These tumors also had a significantly higher mitotic index than those induced by *PDGFB* alone. One explanation for the observed increase in tumor cell proliferation is the commensurate decrease in apoptotic cell death observed in HGGs from the RCAS-*PDGFB* + RCAS-*STAT3* injection set. We found an inverse relationship between CC3 and pSTAT3 expression, which is consistent with our previous studies and confirms that the suppression of apoptosis contributes to the increase in tumor grade. Cumulatively, these data indicate that STAT3 plays a key role in the malignant progression of PDGF-induced glioma.

Recently, a correlation between *STAT3* expression and the mesenchymal phenotype of glioma was reported.[26] As a transcription factor, *STAT3* has been suspected to be a "master regulator" in the transformation of gliomas, from the less aggressive proneural phenotype to the deadlier mesenchymal phenotype.[6,26] At least one other transcriptional activator, *TAZ*, has been shown to facilitate the conversion of gliomas from a proneural to a mesenchymal phenotype.[27] In our study, the level of pSTAT3 expression was found to be significantly higher in mice with shorter tumor latency, suggesting that *STAT3* expression is associated with a more lethal phenotype. Additionally, the key histologic features of mesenchymal glioma (necrosis and microvascular proliferation) were much more common in tumors induced by RCAS-*PDGFB* + RCAS-*STAT3* than in those induced by RCAS-*PDGFB* alone. This was further verified by quantifying the expression of CD31, a marker of microvascular proliferation. We corroborated the histologic observations with additional immunohistochemical staining and showed that a proneural marker, Olig2, was expressed homogeneously throughout high-grade tumors induced by expression of *PDGFB* alone but that Olig2 expression was absent in areas of high-grade histology in gliomas induced by coexpression of *PDGFB* and *STAT3*. Additionally, inhibition of STAT3 expression by the selective STAT3 inhibitor WP1066 resulted in a decrease in the proportion of HGGs in tumor-bearing mice. HGGs from treated mice also demonstrated decreased expression of CD31 compared with HGGs from nontreated mice. Taken together, these data from an in vivo model support the contention that STAT3 acts as a key regulator of the mesenchymal transition.

Signaling through the PDGF receptor is known to induce *STAT3* activation,[28,29] and we detected a low level of pSTAT3 expression in high-grade tumors in mice injected with RCAS-*PDGFB* alone. However, a significantly higher level of pSTAT3 expression was observed in tumors induced by RCAS-*PDGFB* + RCAS-*STAT3* than in tumors induced by RCAS-*PDGFB* alone. pSTAT3-expressing cells also localized to areas of necrotic foci in high-grade tumors. The association of pSTAT3 with necrosis is significant not only because of the relevance with respect to the mesenchymal phenotype, but also because necrosis is independently associated with lower survival rates in human glioma patients.[30] As an alternative explanation, hypoxia, which is known to induce the pSTAT3 pathway[31–33] and is present in areas of necrosis, may also induce pSTAT3 expression via a feed-forward mechanism.

Subclasses of HGG have been defined by activation of specific signal transduction pathways.[18] These subclasses have been further distinguished not only by the signaling pathways that initiate them but also by their phenotypic characteristics. For example, the PDGF signaling pathway is associated with the proneural subclass of HGG and tumors induced by PDGFB using the RCAS/Ntv-a system display proneural features.[6,34] To date, STAT3 has not been shown to have an initiating effect on a specific subclass of HGG, and we were unable to show that independent expression of RCAS-*STAT3* was capable of inducing tumors. However, STAT3 can cause mesenchymal transformation in human glioma stem cell lines, and elimination of STAT3 can decrease mesenchymal differentiation of these same cells.[26] The data obtained in our in vivo model in which *STAT3* was expressed in glioneuronal progenitor cells confirm and extend the observations that *STAT3* may be an important link in a possible proneural to mesenchymal transition. Finally, we also showed that inhibiting STAT3 expression reduces the lethality of the tumor in vivo, verifying it as a rational target in the treatment of glioma. Further investigations into the mechanisms of mesenchymal transformation mediated by *STAT3* will be of use in developing treatments to mitigate the deadly effects of its expression in gliomas.

Supplementary Material

Supplementary material is available at *Neuro-Oncology Journal* online (http://neuro-oncology.oxfordjournals.org/).

Acknowledgments

We thank Audria Patrick, David M. Wildrick, PhD, and Karen Muller, PhD, for editorial assistance.

Conflict of interest statement. None declared.

Funding

This work was supported by the Brain Tumor Society (A.B.H.), the Anthony Bullock III Foundation (A.B.H.), the Mitchell Foundation (A.B.H.), and the Dr Marnie Rose Foundation (A.B.H. and G.R.), National Institutes of Health grants (CA120813 to A.B.H., P50 CA093459 to A.B.H., P50 CA127001 to A.B.H. and G.R., NS070928 to G.R.), and an MD Anderson Cancer Center Support Grant (CA016672).

References

1. Cairncross G, Berkey B, Shaw E, et al. Phase III trial of chemotherapy plus radiotherapy compared with radiotherapy alone for pure and mixed anaplastic oligodendroglioma: Intergroup Radiation Therapy Oncology Group Trial 9402. *J Clin Oncol*. 2006;24:2707–2714.
2. Jaeckle KA, Ballman KV, Rao RD, Jenkins RB, Buckner JC. Current strategies in treatment of oligodendroglioma: evolution of molecular signatures of response. *J Clin Oncol*. 2006;24:1246–1252.
3. Stupp R, Mason WP, van den Bent MJ, et al. Radiotherapy plus concomitant and adjuvant temozolomide for glioblastoma. *N Engl J Med*. 2005;352:987–996.
4. van den Bent MJ, Carpentier AF, Brandes AA, et al. Adjuvant procarbazine, lomustine, and vincristine improves progression-free survival but not overall survival in newly diagnosed anaplastic oligodendrogliomas and oligoastrocytomas: a randomized European Organisation for Research and Treatment of Cancer phase III trial. *J Clin Oncol*. 2006;24:2715–2722.
5. Louis DN, Ohgaki H, Wiestler OD, et al. The 2007 WHO classification of tumours of the central nervous system. *Acta Neuropathol*. 2007;114:97–109.
6. Verhaak RG, Hoadley KA, Purdom E, et al. Integrated genomic analysis identifies clinically relevant subtypes of glioblastoma characterized by abnormalities in PDGFRA, IDH1, EGFR, and NF1. *Cancer Cell*. 2010;17:98–110.
7. Furnari FB, Fenton T, Bachoo RM, et al. Malignant astrocytic glioma: genetics, biology, and paths to treatment. *Genes Dev*. 2007;21: 2683–2710.
8. Shih AH, Holland EC. Platelet-derived growth factor (PDGF) and glial tumorigenesis. *Cancer Lett*. 2006;232:139–147.
9. Appolloni I, Calzolari F, Tutucci E, et al. PDGF-B induces a homogeneous class of oligodendrogliomas from embryonic neural progenitors. *Int J Cancer*. 2009;124:2251–2259.
10. Uhrbom L, Hesselager G, Nister M, Westermark B. Induction of brain tumors in mice using a recombinant platelet-derived growth factor B-chain retrovirus. *Cancer Res*. 1998;58:5275–5279.
11. Dai C, Celestino JC, Okada Y, Louis DN, Fuller GN, Holland EC. PDGF autocrine stimulation dedifferentiates cultured astrocytes and induces oligodendrogliomas and oligoastrocytomas from neural progenitors and astrocytes in vivo. *Genes Dev*. 2001;15:1913–1925.
12. Doucette T, Yang Y, Zhang W, et al. Bcl-2 promotes malignant progression in a PDGF-B–dependent murine model of oligodendroglioma. *Int J Cancer*. 2011;129:2093–2103.
13. Dunlap SM, Celestino J, Wang H, et al. Insulin-like growth factor binding protein 2 promotes glioma development and progression. *Proc Natl Acad Sci USA*. 2007;104:11736–11741.
14. Huse JT, Brennan C, Hambardzumyan D, et al. The PTEN-regulating microRNA miR-26a is amplified in high-grade glioma and facilitates gliomagenesis in vivo. *Genes Dev*. 2009;23:1327–1337.
15. Bromberg JF, Wrzeszczynska MH, Devgan G, et al. Stat3 as an oncogene. *Cell*. 1999;98:295–303.
16. Abou-Ghazal M, Yang DS, Qiao W, et al. The incidence, correlation with tumor-infiltrating inflammation, and prognosis of phosphorylated STAT3 expression in human gliomas. *Clin Cancer Res*. 2008;14: 8228–8235.
17. Bowman T, Broome MA, Sinibaldi D, et al. Stat3-mediated Myc expression is required for Src transformation and PDGF-induced mitogenesis. *Proc Natl Acad Sci USA*. 2001;98:7319–7324.
18. Brennan C, Momota H, Hambardzumyan D, et al. Glioblastoma subclasses can be defined by activity among signal transduction pathways and associated genomic alterations. *PLoS One*. 2009;4:e7752.
19. Phillips HS, Kharbanda S, Chen R, et al. Molecular subclasses of high-grade glioma predict prognosis, delineate a pattern of disease progression, and resemble stages in neurogenesis. *Cancer Cell*. 2006;9:157–173.
20. Sherry MM, Reeves A, Wu JK, Cochran BH. STAT3 is required for proliferation and maintenance of multipotency in glioblastoma stem cells. *Stem Cells*. 2009;27:2383–2392.
21. Holland EC, Hively WP, DePinho RA, Varmus HE. A constitutively active epidermal growth factor receptor cooperates with disruption of G1 cell-cycle arrest pathways to induce glioma-like lesions in mice. *Genes Dev*. 1998;12:3675–3685.
22. Holland EC, Varmus HE. Basic fibroblast growth factor induces cell migration and proliferation after glia-specific gene transfer in mice. *Proc Natl Acad Sci USA*. 1998;95:1218–1223.
23. Colman H, Giannini C, Huang L, et al. Assessment and prognostic significance of mitotic index using the mitosis marker phospho-histone H3 in low and intermediate-grade infiltrating astrocytomas. *Am J Surg Pathol*. 2006;30:657–664.
24. Arai M, Sasaki A, Saito N, Nakazato Y. Immunohistochemical analysis of cleaved caspase-3 detects high level of apoptosis frequently in diffuse large B-cell lymphomas of the central nervous system. *Pathol Int*. 2005;55:122–129.
25. Kong LY, Wu AS, Doucette T, et al. Intratumoral mediated immunosuppression is prognostic in genetically engineered murine models of glioma and correlates to immunotherapeutic responses. *Clin Cancer Res*. 2010;16:5722–5733.
26. Carro MS, Lim WK, Alvarez MJ, et al. The transcriptional network for mesenchymal transformation of brain tumours. *Nature*. 2010;463:318–325.
27. Bhat KP, Salazar KL, Balasubramaniyan V, et al. The transcriptional coactivator TAZ regulates mesenchymal differentiation in malignant glioma. *Genes Dev*. 2011;25:2594–2609.
28. Sachsenmaier C, Sadowski HB, Cooper JA. STAT activation by the PDGF receptor requires juxtamembrane phosphorylation sites but not Src tyrosine kinase activation. *Oncogene*. 1999;18:3583–3592.
29. Vignais ML, Sadowski HB, Watling D, Rogers NC, Gilman M. Platelet-derived growth factor induces phosphorylation of multiple JAK family kinases and STAT proteins. *Mol Cell Biol*. 1996;16:1759–1769.
30. Barker FG, 2nd, Davis RL, Chang SM, Prados MD. Necrosis as a prognostic factor in glioblastoma multiforme. *Cancer*. 1996;77:1161–1166.
31. Wei J, Barr J, Kong LY, et al. Glioma-associated cancer-initiating cells induce immunosuppression. *Clin Cancer Res*. 2010;16:461–473.
32. Jung JE, Lee HG, Cho IH, et al. STAT3 is a potential modulator of HIF-1-mediated VEGF expression in human renal carcinoma cells. *FASEB J*. 2005;19:1296–1298.
33. Noman MZ, Buart S, Van Pelt J, et al. The cooperative induction of hypoxia-inducible factor-1 alpha and STAT3 during hypoxia induced an impairment of tumor susceptibility to CTL-mediated cell lysis. *J Immunol*. 2009;182:3510–3521.
34. Silber J, Jacobsen A, Ozawa T, et al. miR-34a Repression in proneural malignant gliomas upregulates expression of Its Target PDGFRA and Promotes Tumorigenesis. *PLoS One*. 2012;7:e33844.